Effects of Polymorphism on Functional Group Dynamics: Solid State ^{2}H NMR Studies of the Dynamic Properties of the α and β Phases of L-Glutamic Acid

Simon J. Kitchin, Shinbyoung Ahn, and Kenneth D. M. Harris*

School of Chemical Sciences, University of Birmingham, Edgbaston, Birmingham B15 2TT, United Kingdom

Received: January 11, 2002; In Final Form: April 25, 2002

L-Glutamic acid (LGA) exists as two polymorphic solid phases (denoted the α and β phases) with different molecular conformations. This paper investigates the contrasting dynamic properties of the α and β phases of LGA, from measurements of solid state ^{2}H NMR line shapes and spin−lattice relaxation times for the $-ND_3^+$ groups in selectively deuterated samples. For both phases, the ^{2}H NMR line shapes have been simulated successfully in terms of a three-site 120° jump motion of the $-ND_3^+$ group, with the jump frequency varying from 1.5×10^7 to 1.5×10^3 s^{-1} within the temperature range 373 to 198 K. The activation energy for the reorientation of the $-ND_3^+$ group is higher for the α phase [(47 ± 2) kJ mol^{-1}] than for the β phase [(34 ± 3) kJ mol^{-1}]. The ^{2}H NMR spin−lattice relaxation time data are also consistent with the three-site 120° jump motion of the $-ND_3^+$ group and are in good agreement with the activation energies [α phase, (48 ± 1) kJ mol^{-1}; β phase, (39 ± 2) kJ mol^{-1}] determined from our ^{2}H NMR line shape studies. The differences in the dynamic properties of the $-ND_3^+$ groups between the two polymorphs can be rationalized directly in terms of different local environments in the crystal structures, particularly concerning the different hydrogen bonding geometries involving the $-ND_3^+$ groups.

1. Introduction

The phenomenon of polymorphism[1−3] arises when a set of crystalline materials has the same chemical composition but different crystal structures. Thus, in the case of molecular solids, polymorphism arises when a given type of molecule can form different crystal structures. Although the different polymorphs contain the same molecule, the solid state properties of polymorphs should generally be different as a consequence of the different crystal structures. In addition to the major importance of controlling polymorphism within industrial contexts, the phenomenon of polymorphism is of considerable current interest from the academic viewpoint, as comparisons between the properties of polymorphs provide an ideal basis on which to understand relationships between solid state properties and crystal structure. In the present paper, we explore the effects of polymorphism on functional group dynamics in the molecular solid state.

^{2}H NMR spectroscopy is a powerful technique for studying molecular reorientation in solids,[4−11] and has been applied widely to study molecular dynamics in a broad range of materials, including dynamic aspects of phase transitions in solids, the dynamics of guest molecules in solid inclusion compounds, dynamics of hydrogen bonding arrangements, and the motional properties of polymers and membranes. In the case of ^{2}H NMR line shape analysis, the technique is particularly informative when the rate of motion is in the range 10^3 to 10^7 s^{-1}. Faster rates of motion may be probed using ^{2}H NMR spin−lattice relaxation time (T_1) measurements. In this paper, we employ both ^{2}H NMR line shape analysis and ^{2}H NMR spin−lattice relaxation time measurements to investigate the dynamics of the two polymorphs of L-glutamic acid.

* Corresponding author. Telephone: +44-121-414-7474. Fax: +44-121-414-7473. E-mail: K.D.M.Harris@bham.ac.uk.

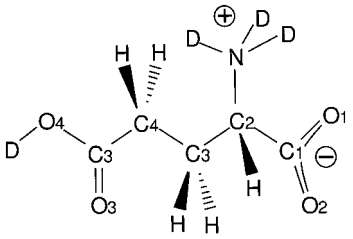

Figure 1. Molecular structure of deuterated L-glutamic acid (LGA-d_4) in the zwitterion form.

L-Glutamic acid (Figure 1; $HO_2CCH_2CH_2CH(NH_2)CO_2H$; abbreviated LGA) exists as two polymorphic solid phases (denoted the α and β phases) that have different molecular conformations and differences in the local hydrogen bonding geometries (see below). The crystal structures of the α phase[12] and the β phase[13] have been determined from single-crystal neutron diffraction data. Both polymorphs crystallize in space group $P2_12_12_1$ with one molecule in the asymmetric unit, and in both cases the LGA molecule exists as the zwitterion [i.e., $HO_2CCH_2CH_2CH(NH_3^+)CO_2^-$]. However, the dynamic properties of the $-NH_3^+$ groups in the two polymorphs may be expected to differ as a consequence of the different local hydrogen bonding geometries and different crystal packing arrangements, both of which may influence the rate and mechanism of motion of the $-NH_3^+$ group. Details of the hydrogen bonding geometries in the α and β phases of LGA polymorphs, as determined from single-crystal neutron diffraction data,[12,13] are shown in Figure 2.

Although there have been some previous solid state NMR studies of the reorientational motion of $-NH_3^+$ groups in amino acids, to our knowledge there have been no previous studies to compare the dynamics of different polymorphs of a given amino acid. Among these previous studies, early ^{2}H NMR investigations of powder[14] and single crystal[15] samples of glycine and

10.1021/jp020064r CCC: $22.00 © 2002 American Chemical Society
Published on Web 07/13/2002

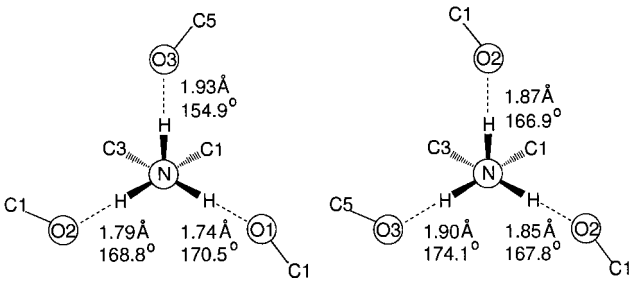

Figure 2. Hydrogen bonding geometries (H···O distances and N−H···O angles) involving the $-NH_3^+$ group for (a) the α phase of LGA and (b) the β phase of LGA, determined at 293 K from single-crystal neutron diffraction data[12,13] of the nondeuterated material.

L-alanine[16] confirmed that the $-NH_3^+$ group undergoes reorientation about the C−N bond. Subsequently, Andrew and coworkers[17−19] used solid state ^{1}H NMR techniques to study molecular motion in polycrystalline samples of a number of amino acids. The reorientation of $-NH_3^+$ groups was found to be an important mechanism for ^{1}H spin−lattice relaxation, and from such studies the activation energies for the reorientation of the $-NH_3^+$ groups in different amino acids were found to fall within the range 28 to 52 kJ mol^{-1}. More recent studies have included detailed ^{2}H NMR analyses of $-ND_3^+$ groups in powder samples of amino acids, including L- and DL-methionine,[20] L-alanine,[21−23] glycine, aspartic acid (DL, D, and L forms) and leucine.[24]

In this paper, solid state ^{2}H NMR line shape analysis and ^{2}H NMR spin−lattice relaxation time measurements for the $-ND_3^+$ groups and $-CO_2D$ groups of the α and β polymorphs of selectively deuterated LGA [$DO_2C(CH_2)_2CH(CO_2^-)ND_3^+$; denoted LGA-$d_4$] are used in order to elucidate differences in the local structural and dynamic properties of these groups in the two polymorphs.

2. Experimental Section

2.1. Sample Preparation. The α and β phases of LGA-d_4 were prepared by crystallization from a saturated solution of LGA in D_2O. Crystals of the α phase were prepared by evaporation at ambient temperature under a stream of dry air, whereas crystals of the β phase were prepared by cooling the solution relatively rapidly from 60 °C to ambient temperature. In some cases, the sample obtained was not a single phase of the required polymorph. However, in such cases the crystals of the α and β phases could be separated by hand under an optical microscope, as the two polymorphs of LGA-d_4 have different crystal morphologies (α phase, prismatic crystals; β phase, needle-like crystals). Powder X-ray diffraction (Siemens D5000 diffractometer; Ge-monochromated $CuK_{\alpha 1}$ radiation) was used to characterize each phase of LGA-d_4 and to confirm prior to the solid state NMR studies that each sample was a single phase of the specified polymorph. Mass spectrometry (VG ZabSpec Mass Spectrometer; FABMS using a cesium ion gun) and infrared absorption spectroscopy (Perkin-Elmer PARAGON 1000 FT-IR spectrometer) confirmed that the level of deuteration in the samples of the α and β phases of LGA-d_4 used for our solid state ^{2}H NMR measurements was close to 100% for both the $-ND_3^+$ and $-CO_2D$ groups.

2.2. Solid State ^{2}H NMR Spectroscopy. All solid state ^{2}H NMR experiments were performed on a Chemagnetics CMX-Infinity 300 spectrometer (^{2}H operating frequency 46.080 MHz) using a Chemagnetics nonspinning probe with 5 mm (i.d.) coil. Spectra were recorded over the temperature range 198 to 373 K using the standard quadrupole echo pulse sequence with an eight step phase cycle and a 90° pulse duration of 2.0 μs. Between 24 and 1000 transients were acquired at each temperature, with recycle delays of at least five times the largest value of $\langle 1/T_1\rangle_p^{-1}$, where $\langle 1/T_1\rangle_p^{-1}$ denotes the powder average ^{2}H NMR spin−lattice relaxation time. At low temperature (below 243 K for the α phase and below 198 K for the β phase), the value of $\langle 1/T_1\rangle_p^{-1}$ for the $-CO_2D$ group was too long to be measured directly, and extrapolated values of $5 \times \langle 1/T_1\rangle_p^{-1}$ were used.

Powder average ^{2}H NMR spin−lattice relaxation times were measured in the temperature range 198 to 373 K using a saturation-recovery pulse sequence with quadrupole echo detection: $[\tau_d-(90°)_x]_n-\tau_r-(90°)_\phi-\tau-(90°)_{\phi\pm\pi/2}-\tau'-$acquire−recycle. The number of 90° pulses used for saturation was typically $n = 30$, with $\tau_d = 250$ μs, $\tau = 30$ μs, and $\tau' < \tau$. The variable relaxation delay τ_r was increased geometrically according to $\tau_r = t_o[(10)^{1/10}]^{N-1}$, where N is the delay number and t_o is the value of the first delay (i.e., $\tau_r = t_o$ for $N = 1$). The number of relaxation delays τ_r used in different experiments was between 31 and 82.

2.3. ^{2}H NMR Line Shape Simulations. ^{2}H NMR line shapes were simulated using the program MXQET.[25] The dynamic model used to describe the motion of the $-ND_3^+$ group in LGA is based on a three-site 120° jump motion about the C(2)−N bond (Figure 1). In each polymorph, the $-ND_3^+$ group has a nonsymmetric environment (i.e., point symmetry lower than C_3) with different geometries for the three N−D···O hydrogen bonds, as shown in Figure 2, corresponding to hydrogen bonds of different strengths. Thus, during the three-site 120° jump motion of the $-ND_3^+$ group, each individual deuteron experiences a hydrogen bond of different geometry and different strength in each of the three positions occupied by the group, but on considering the $-ND_3^+$ group as a whole, the set of three hydrogen bonds formed by the group is identical for each of the three positions occupied by the group during the three-site 120° jump motion (although the identity of the individual deuteron forming each of the three different hydrogen bonds is different for each of the three positions occupied by the group during the motion). Thus, considering the $-ND_3^+$ group as a whole, the three positions occupied by the group during the three-site 120° jump motion must have equal total energy and therefore must represent minima of equal depth. It then follows that the equilibrium populations of all three positions occupied by the group must be equal and that the jump rates from one position to another must also be equal.

In the line shape simulations, the principal component (z-axis) of the electric field gradient (EFG) tensor $\boldsymbol{V}$ for each deuteron site was assumed to be coincident with the N−D bond vector (this assumption is supported by a previous low-temperature single-crystal ^{2}H NMR study of deuterated glycine,[26] which showed that the deviation of the direction of the principal component V_{zz} from the N−D bond direction for the deuterons in an $-ND_3^+$ group is less than 1°). For each phase of LGA, the Euler angle θ relating the principal component of the EFG tensor to the rotation axis (the C(2)−N bond vector) of the $-ND_3^+$ group was taken from the crystal structure determined from single-crystal neutron diffraction data,[12,13] as an average over the three deuteron sites in the group (α phase, $\theta = 70.0°$; β phase, $\theta = 69.0°$).

For each position occupied by the $-ND_3^+$ group during the three-site 120° jump motion, the three deuteron sites are not related by symmetry (in either polymorph) and therefore each deuteron site may, in principle, have different values of the static quadrupole coupling constant χ [$\chi = e^2qQ/h$; QCC] and static

TABLE 1: Values of the Effective Static Quadrupole Coupling Constant (χ^{eff}) and Effective Static Asymmetry Parameter (η^{eff}) Used in the ^{2}H NMR Line Shape Simulations for the $-ND_3^+$ Deuterons in the α and β Phases of LGA-d_4 at Different Temperatures

	α phase		β phase	
T/K	χ^{eff}/kHz	η^{eff}	χ^{eff}/kHz	η^{eff}
373	147	0.25		
358	147	0.25	158	0.11
338	147	0.24	158	0.11
318	147	0.24	158	0.10
298	147	0.23	158	0.09
278	147	0.22	160	0.05
258	150	0.19	160	0.05
238	153	0.18	160	0.05
218			166	0.05
198			166	0.05

asymmetry parameter η [$\eta = (|V_{yy}| - |V_{xx}|)/|V_{zz}|$; where $|V_{zz}| \geq |V_{yy}| \geq |V_{xx}|$]. As a consequence, the ^{2}H NMR line shape in the slow motion limit may, in principle, consist of three overlapping Pake powder patterns with slightly different line shapes, and in the fast motion limit, the motionally averaged asymmetry parameter may be nonzero even though the static asymmetry parameter for each deuteron site may be close to zero. However, even in the spectra recorded at the lowest temperatures studied, separate powder patterns associated with the three deuteron sites of the $-ND_3^+$ group are not resolved. Thus, for each polymorph, the values of the static quadrupole interaction parameters χ and η for each of the three deuteron sites were taken to be equal. As discussed below, the motionally averaged asymmetry parameter was indeed observed to be nonzero in the experimental line shapes, and to take this into account in the line shape simulations, the first and third Euler angles (ϕ and ψ respectively, in the convention of Rose[27]) were chosen such that $\psi = 2\pi - \phi$ (with the effect that the *x* and *y* components of the EFG tensor are not completely averaged to zero by the motion).

In the line shape simulations, the ^{2}H NMR line shape calculated for the motion of the $-ND_3^+$ group was summed with a static line shape representing the $-CO_2D$ group, with a 3:1 scaling to account for the relative numbers of deuterons in the two different types of groups (under the assumption that the level of deuteration was equal for all deuteron sites). Note that the ratio of the integrated intensities of the two sub-spectra is not necessarily 3:1 because of the effects of finite pulse widths and because the intensities of the line shapes can be attenuated by motion in the intermediate regime (10^3 s$^{-1} \lesssim k \lesssim 10^7$ s^{-1}); this latter effect arises when exchange occurs between sites that have different evolution frequencies during the delay periods in the pulse sequence.

The static quadrupole coupling constant and static asymmetry parameter for the $-ND_3^+$ group were initially established from best fits of the spectra recorded at the lowest temperatures. Thus, for the α phase, $\chi = 153.0$ kHz and $\eta = 0.18$ from the spectrum at 238 K, and for the β-phase, $\chi = 166.0$ kHz and $\eta = 0.05$ from the spectrum at 198 K. We note that these measured values of χ and η do not necessarily represent the true static quadrupole coupling constant and static asymmetry parameter, as they subsume the effects of rapid, small-amplitude motions (e.g., librational motions) that may be occurring at these temperatures. For this reason, we describe these values as the "effective" static quadrupole coupling constant and "effective" static asymmetry parameter, denoted χ^{eff} and η^{eff}, respectively. In simulations of the ^{2}H NMR line shape at higher temperatures, χ^{eff} and η^{eff} were allowed to vary slightly (see Table 1) to take account of changes in the rapid, small-amplitude motions with increase of temperature (e.g., increase in amplitude of such motion with increase of temperature). We reiterate that the values of χ^{eff} and η^{eff} used in our spectral simulations represent average values for the three deuteron sites of the $-ND_3^+$ group within the crystal structure, and that the actual values of χ^{eff} and η^{eff} for each individual deuteron site could differ from the average values.

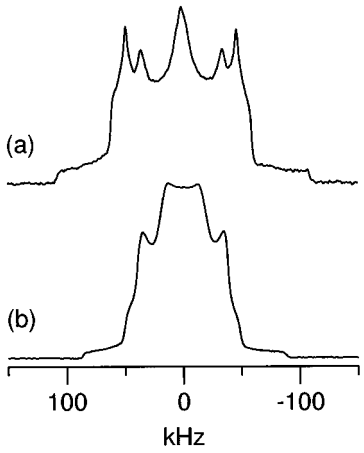

Figure 3. Experimental quadrupole echo ^{2}H NMR spectra for (a) the α phase of LGA-d_4 at 298 K and (b) the β phase of LGA-d_4 at 298 K. Both spectra were recorded with a pulse spacing of 30 μs.

For the $-CO_2D$ group, the effective static quadrupole interaction parameters χ^{eff} and η^{eff} used in our line shape simulations were 143.0 kHz $\leq \chi^{eff} \leq$ 149.0 kHz and $0.06 \leq \eta^{eff} \leq 0.11$ for the α phase and $\chi^{eff} = 116.0$ kHz and $0.12 \leq \eta^{eff} \leq 0.15$ for the β phase. These values are similar to those previously reported for hydrogen bonded $-CO_2D$ groups.[28]

3. Results and Discussion

3.1. Preliminary Observations. The solid state ^{2}H NMR spectra recorded at 298 K for the α and β phases of LGA are shown in Figure 3. For both polymorphs, it is clear that the motion of the $-ND_3^+$ group is in the intermediate regime (motional frequencies in the range 10^3 to 10^7 s^{-1}), in which the line shape is particularly sensitive to the rate of molecular motion, and thus particularly sensitive to temperature. For the α phase, the spectrum is a superposition of two powder patterns, one (containing three maxima toward the center of the spectrum) associated with the $-ND_3^+$ group, and the other (a wider Pake powder pattern) associated with the $-CO_2D$ group. For the β phase, the spectrum consists of a central contribution from the $-ND_3^+$ group and a wider Pake powder pattern for the $-CO_2D$ group. The spectra for the α and β phases are significantly different, indicating clear differences in the dynamics of the $-ND_3^+$ group in the two polymorphs. In addition, differences in the line shapes for the $-CO_2D$ groups reflect different values of the effective static quadrupole interaction parameters for the two polymorphs. A detailed analysis of the ^{2}H NMR line shapes is discussed in section 3.3.

3.2. ^{2}H NMR Spin−Lattice Relaxation Analysis. Powder average ^{2}H NMR spin−lattice relaxation times $\langle 1/T_1 \rangle_p^{-1}$ for the α and β phases of LGA-d_4 were measured over the temperature range 198 to 373 K using the saturation-recovery pulse sequence with quadrupole echo detection. In each phase, the spin−lattice relaxation has two components: a component with shorter spin−lattice relaxation time assigned to the $-ND_3^+$ group, and a component with longer spin−lattice relaxation time assigned to the $-CO_2D$ group. The values of $\langle 1/T_1 \rangle_p^{-1}$ for the two components were obtained from double exponential fits of the

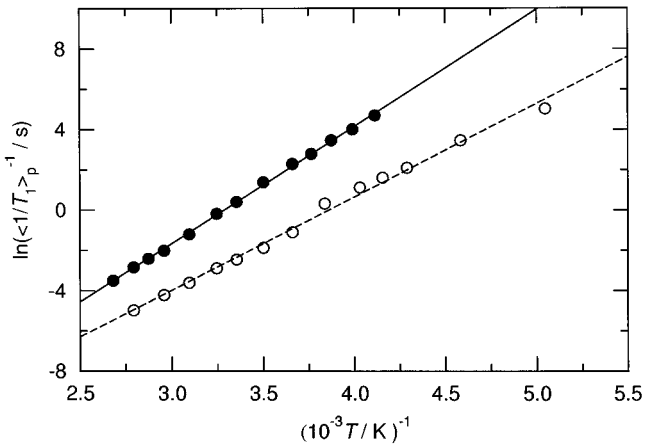

Figure 4. Temperature dependence of the powder-average ^{2}H NMR spin−lattice relaxation time $\langle 1/T_1\rangle_p^{-1}$ for the $-ND_3^+$ deuterons in the α phase (filled circles) and the β phase (open circles) of LGA-d_4.

data from the saturation-recovery experiment at each temperature, and the assignment of each component was based on partially relaxed line shapes obtained from these data.

Figure 4 shows the values of $\langle 1/T_1\rangle_p^{-1}$ for the $-ND_3^+$ group (the component with shorter $\langle 1/T_1\rangle_p^{-1}$) in the α and β phases. As expected for motion in the intermediate regime (10^{-7} s $\lesssim \tau_c \lesssim 10^{-3}$ s), $\langle 1/T_1\rangle_p^{-1}$ decreases as temperature is increased. The minimum in $\langle 1/T_1\rangle_p^{-1}$ (at which the correlation time τ_c is approximately equal to the inverse of the Larmor frequency ω_o) is expected to occur at higher temperature ($T > 373$ K). At each temperature in the range studied, the value of $\langle 1/T_1\rangle_p^{-1}$ is higher for the α phase than the β phase, and the difference in the $\langle 1/T_1\rangle_p^{-1}$ values between the two polymorphs decreases as temperature is increased. Describing the reorientation of the $-ND_3^+$ group as a three-site 120° jump motion with the approximation $\eta = 0$ and with $\omega_o\tau_c \gg 1$, the powder average spin−lattice relaxation time is expressed[29] by

$$\langle 1/T_1\rangle_p = \frac{9\pi^2}{20}\chi^2(\sin^4\theta + \sin^2 2\theta)\frac{1}{\omega_o^2\tau_c} \qquad (1)$$

On the assumption of Arrhenius behavior for the temperature dependence of τ_c [i.e., $\tau_c = \tau_c^o \exp(E_a/RT)$, where τ_c^o is the preexponential factor and E_a is the activation energy], eq 1 can be rearranged to give

$$\ln(\langle 1/T_1\rangle_p^{-1}) = \ln\left(\frac{20\omega_o^2\tau_c^o}{9\pi^2\chi^2(\sin^4\theta + \sin^2 2\theta)}\right) + \frac{E_a}{RT} \qquad (2)$$

The values of τ_c^o and E_a for reorientation of the $-ND_3^+$ group in the α and β phases, obtained by fitting eq 2 to the experimental data, are shown in Table 2. In these calculations, the value of θ was 70.0° for the α phase and 69.0° for the β phase (as discussed in section 2.3), the value of χ was 153 kHz for the α phase and 166 kHz for the β phase (as obtained from the line shape analysis at the lowest temperature studied), and $\omega_o = 2\pi \times 46.080 \times 10^6$ rad s^{-1}.

The activation energy for the reorientation of the $-ND_3^+$ group is higher for the α phase [(48 ± 1) kJ mol^{-1}] than for the β phase [(39 ± 2) kJ mol^{-1}], presumably as a consequence of the different local environments around the $-ND_3^+$ group in the two polymorphs, and may be influenced primarily by differences in the hydrogen bonding geometries. This issue is discussed in more detail in section 4. For comparison, the activation energy for a similar motion in L-alanine has been estimated[22] to be 40.2 kJ mol^{-1}.

TABLE 2: Activation Parameters (E_a and τ_c^o) for the Three-site 120° Jump Motion of the $-ND_3^+$ Group in the α and β Phases of LGA-d_4, Determined from Powder Average ^{2}H NMR Spin−Lattice Relaxation Time Measurements and ^{2}H NMR Line Shape Analysis[a]

	spin−lattice relaxation data		line shape analysis	
	E_a/kJ mol^{-1}	$\ln(\tau_c^o$/s)	E_a/kJ mol^{-1}	$\ln(\tau_c^o$/s)
α phase	48 ± 1	−(32.5 ± 0.3)	47 ± 2	−(32 ± 1)
β phase	39 ± 2	−(31.1 ± 0.8)	34 ± 3	−(29 ± 1)

[a] Note that in the case of the results from line shape analysis, τ_c^o is determined using $\tau_c^o = 1/(3A)$, where A is the pre-exponential factor in the Arrhenius expression for the jump frequency k. The quoted errors in E_a and τ_c^o are derived from the least-squares fitting procedure.

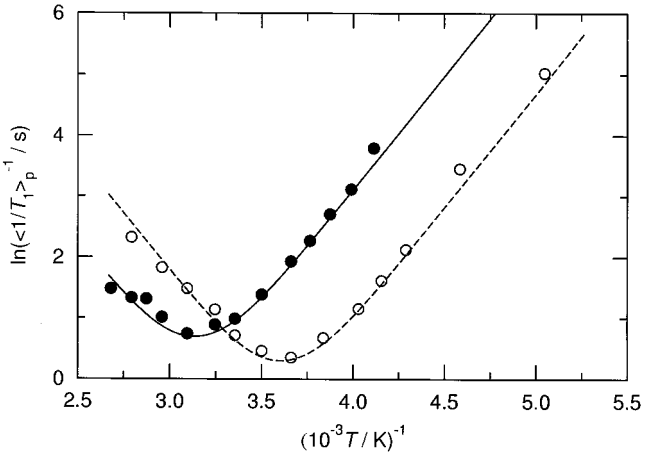

Figure 5. Temperature dependence of the powder-average ^{2}H NMR spin−lattice relaxation time $\langle 1/T_1\rangle_p^{-1}$ for the $-CO_2D$ deuteron in the α phase (filled circles) and the β phase (open circles) of LGA-d_4.

Figure 5 shows the temperature dependence of $\langle 1/T_1\rangle_p^{-1}$ for the $-CO_2D$ group (the component with longer $\langle 1/T_1\rangle_p^{-1}$) in both the α and β phases. Clearly $\langle 1/T_1\rangle_p^{-1}$ varies significantly with temperature and appears to pass through a minimum at about 310 K for the α phase and about 267 K for the β phase. However, because the value of $\langle 1/T_1\rangle_p^{-1}$ for the $-ND_3^+$ group is similar to that for the $-CO_2D$ group at 308 K and lower temperatures, the values of the relaxation times extracted from the double exponential fits in this temperature range are not necessarily reliable. The motion governing the spin−lattice relaxation of the $-CO_2D$ group is probably small-angle libration, and the simplest model to approximate this motion is a two-site jump through a small angle 2δ with equal populations of the two sites. The expression for the powder average spin−lattice relaxation time for this motion, with the approximation $\eta = 0$, is[29]

$$\langle 1/T_1\rangle_p = \frac{9\pi^2}{40}\chi^2\left(\frac{\tau_c}{1+\omega_o^2\tau_c^2} + \frac{4\tau_c}{1+4\omega_o^2\tau_c^2}\right)\sin^2 2\delta \qquad (3)$$

This equation was used to simulate the temperature dependence of $\langle 1/T_1\rangle_p^{-1}$ for the $-CO_2D$ deuterons in both the α and β phases, assuming that the correlation time τ_c has an Arrhenius temperature dependence. The best fits obtained are shown in Figure 5, from which the following parameters have been determined: α phase, $\chi = 149$ kHz, $2\delta = 2.6°$, $E_a = 31$ kJ mol^{-1}, $\tau_c^o = 1.4 \times 10^{-14}$ s; β phase, $\chi = 118$ kHz, $2\delta = 4.0°$, $E_a = 31$ kJ mol^{-1}, and $\tau_c^o = 3.1 \times 10^{-15}$ s. The fact that χ differs substantially between the two polymorphs is a reflection

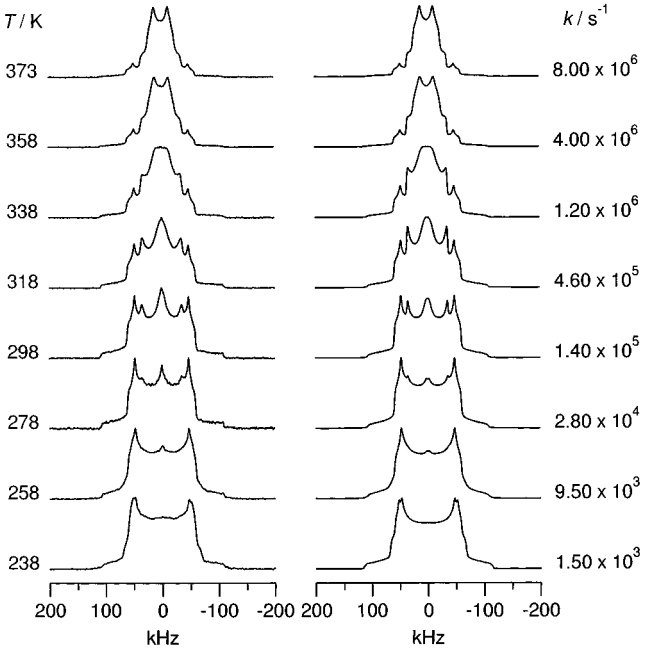

Figure 6. ^{2}H NMR spectra of the α phase of LGA-d$_4$ as a function of temperature and the best-fit simulated spectrum at each temperature (calculated for the dynamic model described in section 2.3).

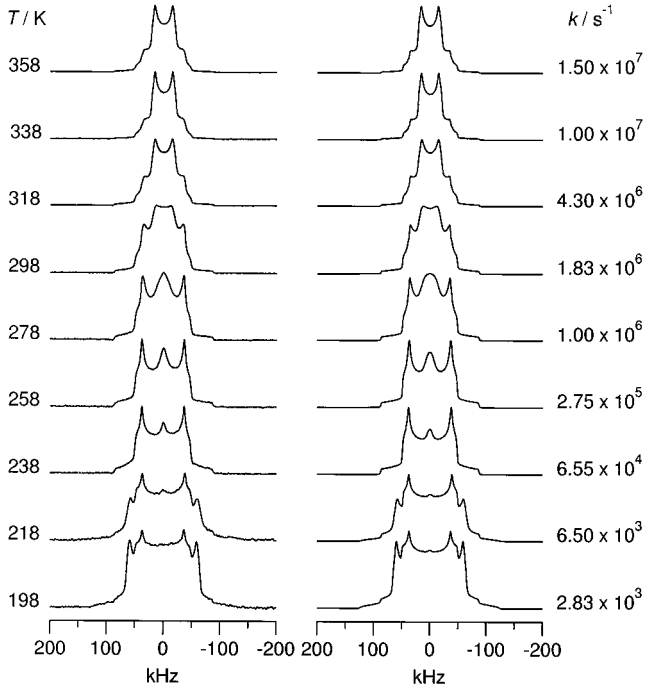

Figure 7. ^{2}H NMR spectra of the β phase of LGA-d$_4$ as a function of temperature and the best-fit simulated spectrum at each temperature (calculated for the dynamic model described in section 2.3).

of the significant differences in hydrogen bonding geometry for the $-CO_2D$ deuterons.[12] In the α phase, the hydrogen atom in the O−H···O hydrogen bond [O−H, 1.024(2) Å; H···O, 1.568(2) Å] lies significantly more unsymmetrically between the two oxygen atoms than in the β phase [O−H = 1.050(4) Å; H···O = 1.475(5) Å], corresponding to a significantly larger component V_{zz} of electric field gradient, and hence a significantly greater value of χ, for the α phase.

3.3. ^{2}H NMR Line Shape Analysis. ^{2}H NMR spectra for the α and β phases of LGA-d$_4$, recorded between 198 and 373 K, are shown in Figures 6 and 7, respectively. The component of the ^{2}H NMR spectrum due to the $-ND_3^+$ group has a significant temperature dependence, with well-defined changes in intensity and line shape, indicating that the reorientation of the $-ND_3^+$ group is in the intermediate motion regime within the temperature range studied. It is clear that the ^{2}H NMR spectra of the α and β phases have different behavior as a function of temperature. For both phases, the component of the spectrum due to the $-CO_2D$ group does not change appreciably with temperature, suggesting that no large amplitude motion of the deuteron in the $-CO_2D$ group occurs (at a frequency greater than 10^3 s^{-1}) within the temperature range investigated. These conclusions are consistent with the spin−lattice relaxation time measurements described above.

^{2}H NMR line shape simulations for a three-site 120° jump motion of the $-ND_3^+$ group and static $-CO_2D$ group were carried out as described in section 2.3, and are compared with the experimental ^{2}H NMR line shapes in Figures 6 and 7. The effective static quadrupole coupling constants used in the simulations for the $-ND_3^+$ deuterons were in the range 147 to 153 kHz for the α phase and 158 to 166 kHz for the β phase, as shown in Table 1. The strength of hydrogen bonding is known to be related to the magnitude of the static quadrupole coupling constant,[30−32] and thus different polymorphs may be expected to have different values of the static quadrupole coupling constant.[33−36] As shown in Table 1, the value of the effective static quadrupole coupling constant χ^{eff} for the $-ND_3^+$ group is lower for the α phase than for the β phase, suggesting that the average strength of the hydrogen bonding involving the $-ND_3^+$ group is greater in the α phase. This issue is discussed in more detail in section 4.

From the simulations of the ^{2}H NMR line shapes, the rate of the three-site 120° jump motion of the $-ND_3^+$ group in the α phase decreases from 8.0×10^6 s^{-1} to 1.5×10^3 s^{-1} on decreasing temperature from 373 to 238 K. The effective static quadrupole coupling constant for the $-ND_3^+$ group (obtained from the best-fit simulations) decreases from 153 to 147 kHz on increasing temperature, reflecting an increase in the amplitude of rapid ($\tau_c \lesssim 10^{-7}$ s) small-amplitude librational motions with increasing temperature (and perhaps small changes in hydrogen bonding geometry). The static asymmetry parameter increases slightly as temperature is increased. Close inspection reveals that the line shapes are slightly nonsymmetric (particularly in the wings of the spectrum), probably due to the effect of the large chemical shift anisotropy[37] of the $-CO_2D$ deuteron.

As shown in Figure 7, the rate of the three-site 120° jump motion of the $-ND_3^+$ group in the β phase decreases from 1.5×10^7 s^{-1} to 2.83×10^3 s^{-1} on decreasing temperature from 358 to 198 K. The effective static quadrupole coupling constant χ^{eff} for the $-ND_3^+$ group decreases from 166 to 158 kHz on increasing temperature, whereas the effective static asymmetry parameter η^{eff} increases as temperature is increased. At each temperature, the rate of reorientation of the $-ND_3^+$ group is significantly higher for the β phase than for the α phase. Above 318 K, the reorientation of the $-ND_3^+$ group in the β phase is in the rapid motion regime. The ^{2}H NMR line shapes for the β phase are also slightly nonsymmetric, probably (as for the α phase) resulting from the large chemical shift anisotropy of the $-CO_2D$ deuteron.

From the best-fit simulated spectrum at each temperature, the rate of reorientation (k) of the $-ND_3^+$ group can be determined as a function of temperature (see Figures 6 and 7), and activation parameters for the motion can be obtained [on the assumption of Arrhenius behavior, i.e., $k = A \exp(-E_a/RT)$] from linear least-squares fits of plots of $\ln(k/s^{-1})$ versus $(T/K)^{-1}$ (Table 2; Figure 8). These fits give

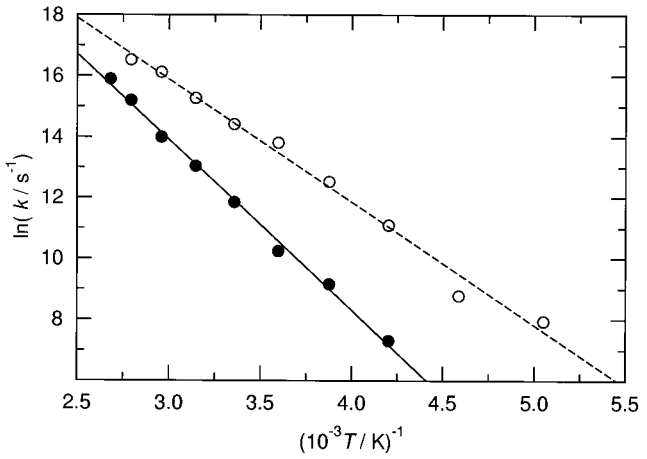

Figure 8. Arrhenius plot for the three-site 120° jump motion of the $-ND_3^+$ group in the α phase (filled circles) and β phase (open circles) of LGA-d_4, determined from best-fit simulations of the ^{2}H NMR line shapes shown in Figures 6 and 7. The straight lines represent linear least-squares fits.

the activation energy E_a as (47 ± 2) kJ mol^{-1} for the α phase and (34 ± 3) kJ mol^{-1} for the β phase, which are within the broad range (ca. 20−60 kJ mol^{-1}) established for reorientation of $-ND_3^+$ groups in other crystalline amino acids.[38] The activation energies derived from the ^{2}H NMR line shape simulations and those derived from our spin−lattice relaxation time measurements (see section 3.2 and Table 2) are in good quantitative agreement (i.e., within the estimated experimental errors).

4. Concluding Remarks

Our ^{2}H NMR studies of the α and β phases of LGA-d_4 have shown that the $-ND_3^+$ group undergoes a 3-site 120° jump motion about the C−N bond, whereas the $-CO_2D$ group does not undergo any large amplitude motion that may be characterized in detail by ^{2}H NMR. Importantly, we have found that the rate of reorientation of the $-ND_3^+$ group has a different temperature dependence for the α and β phases, which undoubtedly reflects the geometric differences in the local interactions involving this group in the two polymorphs. The hydrogen bonding geometries involving the $-ND_3^+$ group in each polymorph (determined from neutron diffraction and therefore implying reliable determination of the hydrogen atom positions) are shown in Figure 2. On the basis of the H···O distances and N−H···O angles shown in Figure 2, we may reasonably infer that the $-NH_3^+$ group is engaged in stronger hydrogen bonding in the α phase than in the β phase, recalling that shorter H···O distances and N−H···O angles closer to 180° are generally indicative of stronger hydrogen bonding. The fact that the average H···O distance for the $-NH_3^+$ group is lower for the α phase (and in particular, two H···O distances for the α phase are shorter than any of the H···O distances for the β phase) provides structural evidence that the $-NH_3^+$ group in the α phase is overall engaged in stronger hydrogen bonding than in the β phase. As now discussed, our solid state ^{2}H NMR results provide clear support for this assertion.

First, the effective static quadrupole coupling constant for the $-ND_3^+$ deuterons obtained from our ^{2}H NMR line shape analysis is smaller for the α phase (147−153 kHz) than for the β phase (158−166 kHz). We recall that these effective static quadrupole coupling constants represent an average over the three deuteron sites for the $-ND_3^+$ group, and therefore may be taken to reflect the overall strength of hydrogen bonding involving the group.

Second, the activation energy for reorientation of $-ND_3^+$ group is found to be higher for the α phase [(47 ± 2) kJ mol^{-1} (line shape analysis); (48 ± 1) kJ mol^{-1} (spin−lattice relaxation data)] than for the β phase [(34 ± 3) kJ mol^{-1} (line shape analysis); (39 ± 2) kJ mol^{-1} (spin−lattice relaxation data)]. Clearly the energy barrier for reorientation of the $-ND_3^+$ group may be expected to depend significantly on the nature of the hydrogen bonding interactions involving this group, and the higher activation energy for the α phase is again consistent with the suggestion that the hydrogen bonding is stronger in this phase. For comparison, the energy barrier for reorientation of the $-ND_3^+$ group in isolated LGA in the gas phase is only about 6 to 15 kJ mol^{-1},[39,40] reflecting the absence of intermolecular hydrogen bonding interactions, and the energy barrier for reorientation of the methyl groups (which do not engage in strong hydrogen bonds) in crystalline amino acids is only about 8 to 20 kJ mol^{-1}.[33,34,41,42]

The results reported in this paper demonstrate the ability and scope of solid state ^{2}H NMR techniques to elucidate differences in functional group dynamics between polymorphic systems and emphasize that, even when the local structural differences between polymorphs may be comparatively minor (in the present case, the $-NH_3^+$ groups in the two polymorphs both engage in three N−H···O hydrogen bonds, albeit of different strengths), significant differences in dynamic properties may nevertheless be observed.

References and Notes

(1) Dunitz, J. D. *Pure Appl. Chem.* **1991**, *63*, 177.
(2) Caira, M. R. *Top. Curr. Chem.* **1998**, *198*, 164.
(3) Bernstein, J.; Davey, R. J.; Henck, J.-O. *Angew. Chem. Int. Ed. Engl.* **1999**, *38*, 3441.
(4) Seelig, J. *Quart. Rev. Biophys*. **1977**, *10*, 353.
(5) Jelinski, L. W. *Annu. Rev. Mater. Sci*. **1985**, *15*, 359.
(6) Alam, T. M.; Drobny, G. P. *Chem. Rev*. **1991**, *91*, 1545.
(7) Vold, R. R.; Vold, R. L. *Adv. Magn. Opt. Reson*. **1991**, 85.
(8) Hoatson, G. L.; Vold, R. L. *NMR Basic Principles and Progress*, Springer-Verlag: Berlin, 1994; Vol. 32, pp 3−67.
(9) Vold, R. R. *Nuclear Magnetic Resonance Probes of Molecular Dynamics*; Tycko, R. Ed.; Kluwer Academic Publishers: Dordrecht, 1994; pp 27−106.
(10) Aliev, A. E.; MacLean, E. J.; Harris, K. D. M.; Kariuki, B. M.; Glidewell, C. *J. Phys. Chem. B* **1998**, *102*, 2165.
(11) Bach-Vergés, M.; S. Kitchin, J.; Harris, K. D. M.; Zugic, M.; Koh, C. A. *J. Phys. Chem. B* **2001**, *105*, 2699.
(12) Lehmann, M. S.; Nunes, A. C. *Acta Crystallogr. B* **1980**, *36*, 1621.
(13) Lehmann, M. S.; Koetzle, T. F.; Hamilton, W. C. *J. Cryst. Mol. Struct*. **1972**, *2*, 225.
(14) Vijayaraghavan, R.; Saraswati, V. *J. Phys. Soc. Jpn.* **1965**, *20*, 2290.
(15) Derbyshire, W.; Gorvin, T.; Warner, D. *Mol. Phys.* **1967**, *12*, 299.
(16) Warner, D.; Gorvin, T.; Derbyshire, W. *Mol. Phys.* **1968**, *14*, 281.
(17) Andrew, E. R.; Hinshaw, W. S.; Hutchins, M. G.; Sjöblom, R. O. I. *Mol. Phys.* **1976**, *31*, 1479.
(18) Andrew, E. R.; Hinshaw, W. S.; Hutchins, M. G.; Sjöblom, R. O. I. *Mol. Phys.* **1977**, *34*, 1695.
(19) Andrew, E. R.; Green, T. J.; Hoch, M. J. R. *J. Magn. Reson.* **1978**, *29*, 331.
(20) Keniry, M. A.; Rothgeb, T. M.; Smith, R. L.; Gutowsky, H. S.; Oldfield, E. *Biochemistry* **1983**, *22*, 1917.
(21) Long, J. R.; Sun, B. Q.; Bowen, A.; Griffin, R. G. *J. Am. Chem. Soc*. **1994**, *116*, 11950.
(22) Williams, M. A. K.; Keenan, R. D.; Halstead, T. K. *Solid State NMR* **1996**, *6*, 47.
(23) Kristensen, J. H.; Hoatson, G. L.; Vold, R. L. *J. Chem. Phys.* **1999**, *110*, 4533.
(24) Gu, Z.; Ebisawa, K.; McDermott, A. *Solid State NMR* **1996**, *7*, 161.
(25) Greenfield, M. S.; Ronemus, A. D.; Vold, R. L.; Vold, R. R.; Ellis, P. D.; Raidy, T. R. *J. Magn. Reson*. **1987**, *72*, 89.
(26) Müller, C.; Schajor, W.; Zimmermann, H.; Haeberlen, U. *J. Magn. Reson*. **1984**, *56*, 235.
(27) Rose, M. E. *Elementary Theory of Angular Momentum*; Wiley: New York, 1957.
(28) Chiba, T.; Soda, G. *Bull. Chem. Soc. Jpn.* **1971**, *44*, 1703.
(29) Alam, T. M.; Drobny, G. P. *Chem. Rev*. **1991**, *91*, 1545.

(30) Sternberg, U.; Brunner, E. *J. Magn. Reson*. **1994**, *108*, 142.
(31) Chiba, T. *J. Chem. Phys*. **1964**, *41*, 1352.
(32) Larsson, K.; Tegenfeld, J.; Hermansson, K. *J. Chem. Soc., Faraday Trans*. **1991**, *87*, 1193.
(33) Batchelder, L. S.; Nin, C. H.; Torchia, D. A. *J. Am. Chem. Soc*. **1983**, *105*, 2228.
(34) Andrew, E. R.; Hinshaw, W. S.; Hutchins, M. G.; Sjöblom, R. O. I.; Canepa, P. C. *Mol. Phys*. **1976**, *32*, 795.
(35) Berglund, B.; Vaughan, R. W. *J. Chem. Phys.* **1980**, *73*, 2037.
(36) Camus, S.; Harris, K. D. M.; Johnston, R. L. *Chem. Phys. Lett*. **1997**, *276*, 186.
(37) DiNatale, J. A.; Vold, R. R. *J. Magn. Reson*. **1995**, *117*, 304.
(38) Keniry, M. A.; Smith, R. L.; Gutowsky, H. S.; Oldfield, E. *Structure and Dynamics: Nucleic Acids and Proteins*; Clementi, E., Sarma, R. H., Eds.; Adenine Press: New York, 1983.
(39) Schmuttenmaer, C. A.; Loeser, J. G.; Saykally, R. J. *J. Chem. Phys*. **1994**, *101*, 139.
(40) Forest, S. E.; Kuczkowski, R. L. *Chem. Phys. Lett*. **1994**, *218*, 349.
(41) Beshah, K.; Olejniczak, E. T.; Griffin, R. G. *J. Chem. Phys*. **1987**, *86*, 4730.
(42) Keniry, M. A.; Kintanar, A.; Smith, R. L.; Gutowsky, H. S.; Oldfield, E. *Biochemistry* **1984**, *23*, 288.